RESEARCH ARTICLE | APRIL 12 2018

A high-performance polydimethylsiloxane electrospun membrane for cell culture in lab-on-a-chip *⊙*

Hajar Moghadas [®] ; Mohammad Said Saidi **™** ; Navid Kashaninejad [®] ; Nam-Trung Nguyen **™** [®]



Biomicrofluidics 12, 024117 (2018) https://doi.org/10.1063/1.5021002





Articles You May Be Interested In

Nanochannels fabricated in polydimethylsiloxane using sacrificial electrospun polyethylene oxide nanofibers

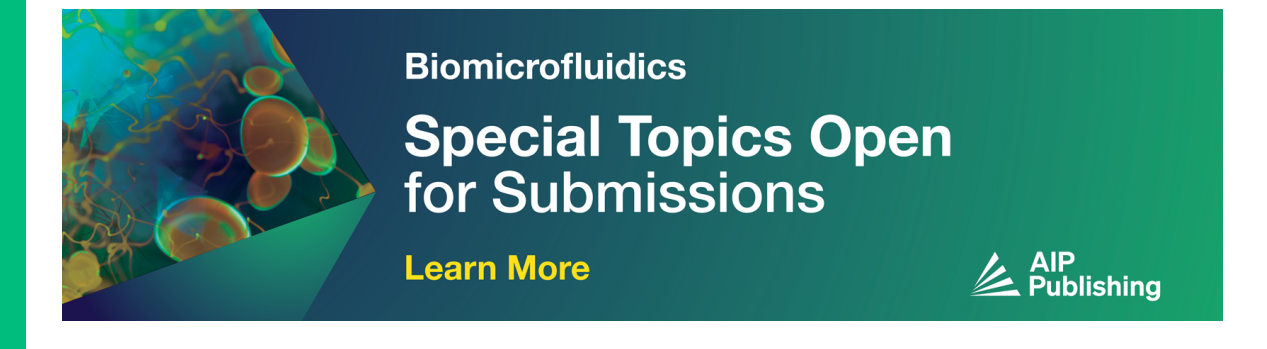
J. Vac. Sci. Technol. B (September 2008)

Optical fiber ultrasound transmitter with electrospun carbon nanotube-polymer composite

Appl. Phys. Lett. (June 2017)

A method to integrate patterned electrospun fibers with microfluidic systems to generate complex microenvironments for cell culture applications

Biomicrofluidics (June 2012)







A high-performance polydimethylsiloxane electrospun membrane for cell culture in lab-on-a-chip

Hajar Moghadas, ¹ Mohammad Said Saidi, ^{1,a),b)} Navid Kashaninejad, ^{2,b)} and Nam-Trung Nguyen^{2,a)}

¹School of Mechanical Engineering, Sharif University of Technology, Tehran, Iran ²Queensland Micro- and Nanotechnology Centre, Nathan Campus, Griffith University, 170 Kessels Road, Brisbane QLD 4111, Australia

(Received 30 December 2017; accepted 2 April 2018; published online 12 April 2018)

Thin porous membranes are important components in a microfluidic device, serving as separators, filters, and scaffolds for cell culture. However, the fabrication and the integration of these membranes possess many challenges, which restrict their widespread applications. This paper reports a facile technique to fabricate robust membrane-embedded microfluidic devices. We integrated an electrospun membrane into a polydimethylsiloxane (PDMS) device using the simple plasma-activated bonding technique. To increase the flexibility of the membrane and to address the leakage problem, the electrospun membrane was fabricated with the highest weight ratio of PDMS to polymethylmethacrylate (i.e., 6:1 w/w). The membrane-integrated microfluidic device could withstand a flow rate of up to 50 µl/min. As a proof of concept, we demonstrated that such a compartmentalized microfluidic platform could be successfully used for cell culture with the capability of providing a more realistic in vivo-like condition. Human lung cancer epithelial cells (A549) were seeded on the membrane from the top microchannel, while the continuous flow of the culture medium through the bottom microchannel provided a shear-free cell culture condition. The tortuous micro-/nanofibers of the membrane immobilized the cells within the hydrophobic micropores and with no need of extracellular matrix for cell adhesion and cell growth. The hydrophobic surface conditions of the membrane were suitable for anchorage-independent cell types. To further extend the application of the device, we qualitatively showed that rinsing the membrane with ethanol prior to cell seeding could temporarily render the membrane hydrophilic and the platform could also be used for anchorage-dependent cells. Due to the three-dimensional (3D) topography of the membranes, three different configurations were observed, including individual single cells, monolayer cells, and 3D cell clusters. This cost-effective and robust compartmentalized microfluidic device may open up new avenues in translational medicine and pharmacodynamics research. Published by AIP Publishing. https:// doi.org/10.1063/1.5021002

I. INTRODUCTION

Membrane technology and microfluidics have been widely used in various biological applications.

Thin porous membranes have been successfully integrated into microfluidic devices for cell culture.

The two types of membranes that have been often used in lab-on-chip applications are polydimethylsiloxane (PDMS) and commercially available membranes. Common commercial membranes are Cyclopore

polycarbonate (PC), thin and transparent Cyclopore PC, Nucleopore

Nucleopore

track-etched PC, and polyethylene terephthalate (PET) membranes. However, these membranes have a number of limitations, which hinder their widespread use in routine cell

a) Authors to whom correspondence should be addressed: mssaidi@sharif.edu and nam-trung.nguyen@griffith.edu.au

b)M. S. Saidi and N. Kashaninejad contributed equally to this work.

culture platforms. For instance, the fabrication process of the master mold for PDMS soft lithography is relatively complicated and requires expensive equipment. Furthermore, both PDMS and commercial membranes fail to provide three-dimensional (3D) physiological conditions required for cell culture because these membranes have a planar two-dimensional (2D) surface. In addition, these membranes need special surface treatment such as coating with extracellular matrix (ECM) to promote cell attachment. PDMS

Recently, researchers have shown increasing interest in applying electrospun membranes (ESMs) in biomedical applications ^{13,14} and tissue engineering. ¹⁵ An ESM consists of micro-/nano-fibers randomly collected on each other to provide a 3D morphological structure. The fabrication technology of ESMs requires straightforward and inexpensive equipment, making it accessible to any laboratory. ^{16–19} More importantly, the physical properties of ESM such as fiber diameter, porosity, thickness, and mechanical strength can be tuned easily and rapidly. ^{14,19} Due to the high surface area to volume ratio of ESMs and the 3D topography of the micro-/nanofibers, ESMs are better candidates for *in vitro* cell culture applications compared to their 2D planar counterparts. Also, ESMs can sufficiently mimic *in vivo* morphological and physiological conditions. ²⁰

Although several studies have investigated cell growth on ESMs, very few works have employed ESMs for cell culture in microfluidic devices. ^{21–24} The most likely reason is the difficulty in integrating ESMs within the microchip without leaking. Higuita-Castro et al. fabricated a biodegradable ESM by mixing polycaprolactone with gelatin and sandwiched the ESM between two PDMS microchannels. 21 However, degradation of the membrane materials may limit further biological assays for long-term culture. Liu et al. used scotch tape to incorporate the electrospun scaffolds made of either polyvinylidene difluoride (PVDF) or PC into a PDMS microchip.²² Although the reversible assembly provided proper sealing for the hydrophobic PVDF scaffold, the bonding was not strong enough to prevent leakage from the hydrophilic PC scaffold. Therefore, this method is not appropriate for incorporating hydrophilic cell culture scaffolds into microfluidic devices. Jo et al. used large mats of electrospun fibers in a microchip and sealed the channels by press-fitting with four clips.²³ Although the press-fitting method can produce a relatively tight bond, unlike the plasma treatment, the bonding is not strong enough to support a high hydrodynamic pressure.²⁴ Wallin et al. directly electrospun the fibers onto a glass slide and bonded the slide irreversibly to a PDMS microchip. However, this method cannot support thick mats of more than $5 \mu m$ because the mats are located in the center of the probing channel and significantly affect the flow field.²⁴ Furthermore, this device fails to provide a shear-free condition for cells. Shear stress of the continuous flow acting on the cultured cells activates the signaling pathways, resulting in cell proliferation, ²⁵ differentiation, ²⁶ adhesion,²⁷ and migration.²⁸ Depending on the desired application, such shear stress can be either favorable or unfavorable. Notably, it is undesirable in chemotaxis assays where the fluid flow pushes cells downstream and moves the cells away from their initial position.²⁹

To solve the challenging task of manufacturing and integrating thin membranes into a microdevice, we employ a facile electrospinning method to produce a hydrophobic membrane and efficiently integrate the membrane in a microfluidic device. For cell culture application, such a microfluidic system can better resemble the complex *in vivo* conditions. To the best of our knowledge, this is the first time that this type of ESM is integrated into a microfluidic-based cell culture platform. In our previous work, we thoroughly explained the detailed fabrication and characterization of such ESM, where the highly hydrophobic ESM was used for the generation of various cell aggregates. ¹⁹ In the present study, we utilized this flexible and robust ESM as a scaffold to provide a shear-free cell culture condition in a microchip. In the proposed platform, one microchannel transports the culture media or reagents, while the other channel provides a shear-free environment for the cell culture. If necessary, the design also allows the flow to pass through the cells and introduce shear stress.

Here, we first evaluated the possibility of cell culture on the ESM made of PDMS and polymethylmethacrylate (PMMA) with a high PDMS content in a 24-well non-treated plate. We then demonstrated the growth of epithelial cells on the ESM embedded into a microfluidic device. Furthermore, the shrinkage of the ESM in the ethanol/water mixture at room temperature was investigated in detail by Fourier transform infrared (FTIR) spectroscopy. The

fabricated ESM is highly hydrophobic and is suitable for anchorage-independent cell adhesion.³⁰ Interestingly, we qualitatively show that by rinsing with ethanol, the ESM becomes hydrophilic. Thus, the proposed platform is suitable for studying both anchorage-independent and anchorage-dependent cells. Most importantly, cell culture is feasible on such a scaffold without any physical or chemical surface treatment processes³¹ such as coating with costly ECM proteins³² and oxygen plasma. Treating the cell culture scaffold with plasma may melt the fibers and change the porosity of the ESM.³³

II. MATERIALS AND METHODS

A. Fabrication of the membrane using the electrospinning technique

The fabrication process of the ESM was thoroughly described in our previous work 19 and is shown schematically in Figs. 1(a) and 1(b). In brief, the prepared solution was extruded from the needle tip with a flow rate of 1 ml/h. Subsequently, a direct current (DC) power supply provided an 18 kV voltage difference to the erupted liquid, and the produced fibers were formed on an aluminum foil collector located 15 cm away from the needle tip. Since direct electrospinning of PDMS is not possible, a carrier polymer with a proper solvent should be utilized. To this aim, PMMA ($M_w = 350~000$ - Sigma-Aldrich) was selected for the electrospinning process of PDMS (Sylgard 184, Sigma-Aldrich). First, PMMA powder should be dissolved in a proper solvent. Accordingly, a mixture of tetrahydrofuran (THF) and dimethylformamide (DMF) (Merck KGaA, Darmstadt, Germany) was chosen due to its compatible solubility with both PDMS and PMMA, as reported previously.³⁴ Therefore, we had to optimize the weight ratio of the two solutions, i.e., THF:DMF as a solvent, as well as the weight ratio of PDMS:PMMA (dissolved in THF and DMF). We found that the weight ratios of 2:1 THF:DMF for the solvent and 6:1 for PDMS:PMMA would lead to the best results [Fig. 1(b)]. We also observed that by changing the duration of the electrospinning process, the thickness of the ESM could be modified. For instance, the membrane thickness was found to be $20 \,\mu m$ when the electrospinning time was $10 \, min$. By increasing the processing time to 60 min, the membrane thickness increased to $100 \, \mu m$.

B. ESM shrinkage

Although the membranes fabricated using the electrospinning technique offer several advantages, shrinkage and deformity of such membranes are their weak points. Shrinkage and deformity of the ESM can significantly affect cell adhesion and proliferation. Accordingly, the extent of ESM shrinkage needs to be quantified carefully. To this aim, 24 square and rectangular pieces of the ESM with various sizes were immersed in 70% ethanol. The containers were carefully sealed to prevent evaporation and shaken manually to allow 70% ethanol completely diffuse into the ESM. The shrinkage was observed within the first 2 min and gradually continued. After 24 h, ethanol was discarded gently, and the samples were allowed to dry at room temperature. The difference between the area of each piece before and after immersing in ethanol was calculated, and the average was reported as the extent of ESM shrinkage. Detailed investigations of the changes in the chemical composition of the ESM due to rinsing with alcohol were carried out by FTIR using a Spectrum RX I (PerkinElmer, USA) with 21 scans at a resolution of 4 cm⁻¹.

C. Fabrication of the microfluidic device

The microfluidic device consisted of an ESM, which was sandwiched between two PDMS microchannels, and had a cell culture chamber with dimensions of $10\,\mathrm{mm}$ (length) $\times 1\,\mathrm{mm}$ (width) $\times 300\,\mu\mathrm{m}$ (height) [Fig. 1(c)]. The master mold of the microchannels was fabricated using precision plastic micromachining. Considering the dimensions of the microfluidic device, this technique is more practical than the conventional silicon-based photolithography method which is more expensive and requires cleanroom facilities. First, the patterns of the microchannels were machined on Plexiglas acrylic PMMA using computer numerical control (CNC) micromilling. Next, the PDMS pre-polymer was mixed with its curing agent at a weight ratio of 10:1 and poured onto the PMMA mold. The system was degassed in a vacuum pump for

30 min and baked for 2 h at 75 °C. Then, the replicated PDMS with the microchannel structures was peeled off from the mold and cut into the required sizes with a razor blade. Subsequently, a biopsy punch was used to create the corresponding inlets and outlets of the device. Finally, it was thoroughly washed with isopropyl alcohol (IPA) and dried with an air gun.

D. ESM assembly on a microchip

First, a portion of the ESM was precisely cut to cover the culture chamber area. The inner surfaces of the top and bottom layers of the microchip were then treated with oxygen plasma for 15 s. Within 2 min, the ESM was sandwiched between the plasma-treated PDMS layers as shown in Fig. 1(c). The microchip was placed directly on a heater at 65 °C for 20 min under a mass of 0.375 kg to increase the bonding strength.

E. Cell culture on the ESM located in a conventional 24-well plate

To investigate and compare the cell culture conditions on the ESM, human lung cancer epithelial cells (A549) were cultured on such membranes. The A549 cell line is broadly utilized to

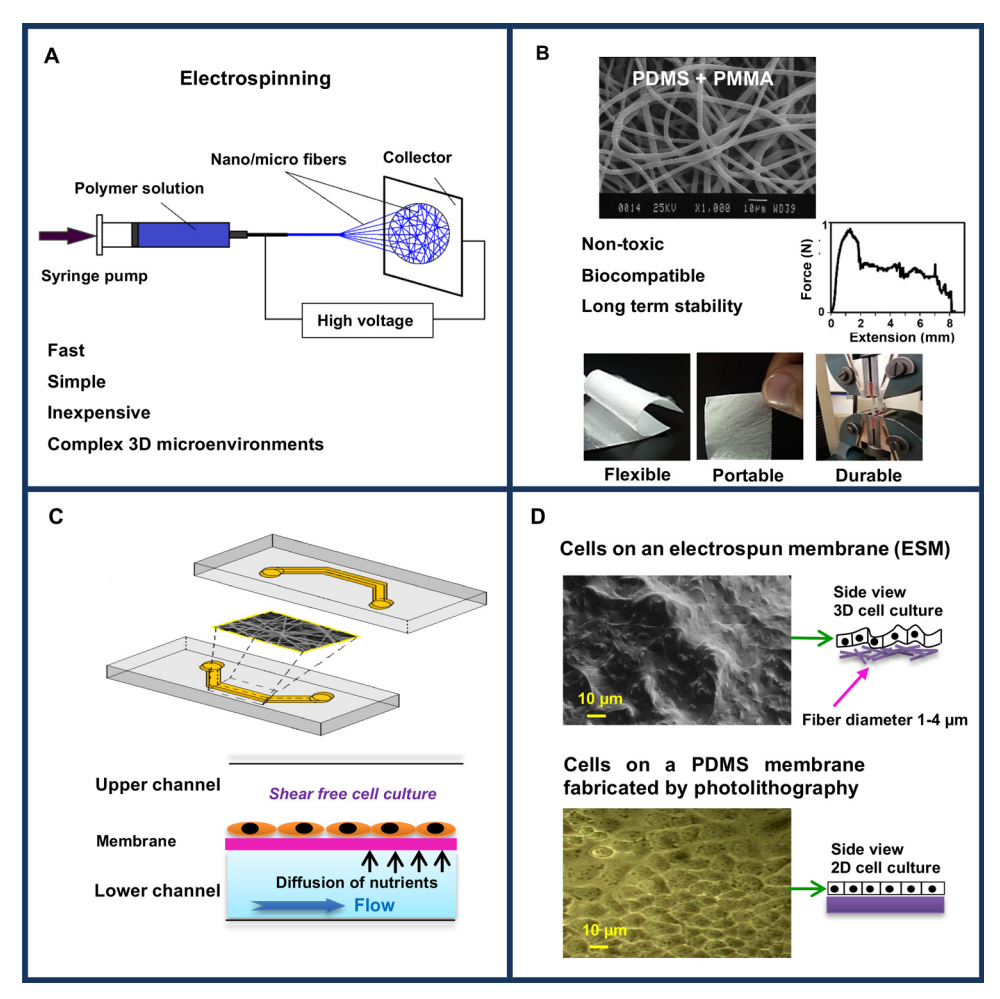


FIG. 1. An electrospun membrane (ESM) as the scaffold for cell culture in lab-on-a-chip: (a) The schematic of the electrospinning technique to fabricate the ESM. The micro-/nanofibers are collected on each other and produce complex 3D matrices. (b) Characterization of the fabricated ESM with high-content PDMS. The ESM is flexible, portable, and durable. (c) In the present study, the ESM is sandwiched between two PDMS microchannels. This membrane separates these microchannels and provides a shear-free cell culture scaffold. (d) Comparison of the cell culture conditions on the ESM and smooth PDMS membrane. Due to the roughness and the heterogeneity of the ESM, it can provide a 3D-like scaffold for cell culture application.

model the alveolar lung cells for drug screening and forms a monolayer structure in vitro.35 Likewise, the alveolar lung cells also form a monolayer configuration in the body. Since the structure of lung alveoli is not smooth, it is expected that cells cultured on the rough ESM can better recapitulate the in vivo morphology of the alveolar lung cells. Therefore, this cell line was selected for the study. As shown in Fig. 1(d), compared to a smooth PDMS membrane, ESM may lead to entirely different cell aggregates. In this study, the ESMs with the cultured cells were tested in both static (conventional 24-well plate) and dynamic (microchip) platforms. To evaluate the cell culture condition in a static platform, first, several pieces of the ESM with dimensions of $0.5 \, \text{cm} \times 0.5 \, \text{cm}$ were sterilized with 96% ethanol and then washed twice with phosphate-buffered saline (PBS). These pieces were immersed in the culture medium [Dulbecco's Modified Eagle's medium, DMEM: F12 (1:1), Bioidea] supplemented with 10% fetal bovine serum (FBS) (Bioidea), 100 unit/ml penicillin, and 100 µg/ml streptomycin (Sigma-Aldrich) and incubated for contamination testing. After 2 days, the culture medium was discarded, and 48 μ l of the cell suspension with a concentration of 1×10^6 cells/ml was added to each portion of the ESM located in the conventional 24-well plate. After 2 h, 952 µl of the culture medium containing 15% FBS was gently added to each well and then incubated. The culture medium was exchanged every 24 h. Accordingly, the total number of cells in each well was fixed at 48 000 cells. To evaluate the cell growth and survival, a 3-(4,5-dimethylthiazol-2yl)-2,5-diphenyltetrazolium bromide (MTT) assay was carried out on the second, fourth, and sixth days. The cell morphology was observed using a scanning electron microscope (SEM) (Leica 440) at a working distance of 39 mm and an accelerating voltage of 25 kV. To stabilize the cells, the ESM was washed twice with PBS and incubated in 4% glutaraldehyde for 4h with and without ethanol fixation.

F. Cell culture on the ESM-integrated microfluidic device

The microchannels were first washed with ethanol (70% or 96% diluted in distilled water) to make the ESM hydrophilic (proper for the cell attachment) and then rinsed carefully with PBS and filled with the culture medium. After 2 h, a cell suspension with a density of 1×10^6 cells/ml was gently injected into the ESM-integrated microfluidic device. The cells were seeded on the ESM from the upper channel, and the culture medium was passed through the lower microchannel. Then, the inlet and the outlet ports of the upper channel were closed. The microchip was aseptically placed in an incubator, while fresh culture medium was pumped through the lower channel continuously with a flow rate of $1 \mu l/min$. Depending on the experiment, the duration of culture medium pumping varied from 12 h to 120 h. Several experiments were also conducted on the microchip without ethanol rinsing to investigate the effect of hydrophobicity of the ESM on the cell morphology.

III. RESULTS AND DISCUSSION

A. ESM shrinkage

The ESM resisted the penetration of the culture medium because it was relatively hydrophobic with an apparent contact angle of $138^{\circ} \pm 2$ for a 3 μ l distilled water droplet [Fig. 2(a), inset left]. However, the ethanol/water mixture could easily penetrate thoroughly and exhibited a small contact angle of $37^{\circ} \pm 2$ on the surface of the ESM [Fig. 2(a), inset right]. Washing with the ethanol/water mixture rendered the ESM hydrophilic and permeable for both distilled water and the culture medium. On the other hand, when the ESM was in contact with 70% ethanol, it shrank significantly. More than $70 \pm 4\%$ shrinkage relative to the initial dimension was observed after overnight dipping [Fig. 2(b)]. The SEM images illustrate the surface morphology of the ESM located in a Petri dish before [Fig. 2(a)] and after [Fig. 2(b)] immersion in 70% ethanol for 24 h at room temperature. The PMMA is dissolved in the ethanol/water mixture and would fill the pores of the ESM. Consequently, the ESM lost its porosity when placed in a conventional Petri dish and washed with 70% ethanol [Fig. 2(b)]. Because PMMA is insoluble in pure ethanol at room temperature, 37 the ESM was rinsed with 96% ethanol and immediately

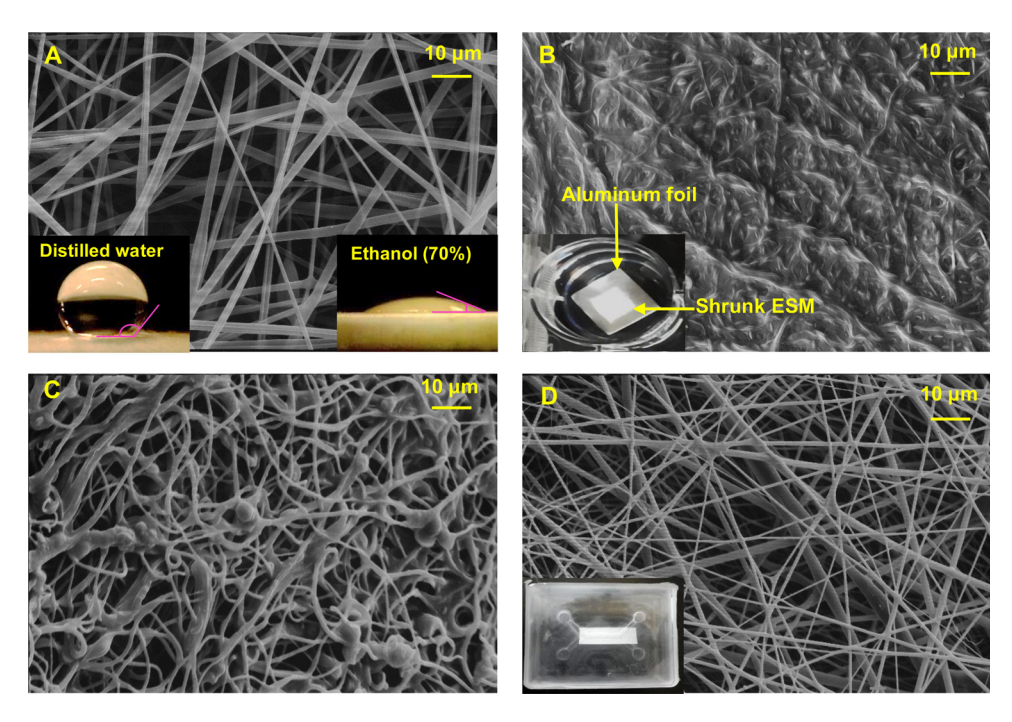


FIG. 2. The effect of ethanol on the ESM shrinkage and deformability. (a) The fibers of an untreated ESM. The fibers are roughly smooth and homogenous. The insets in the figure illustrate the contact angles of water and ethanol on the untreated ESM. Distilled water makes a large contact angle $(138^{\circ}\pm2)$ with the ESM surface. Conversely, the water/ethanol mixture (70% ethanol) makes a small contact angle $(37^{\circ}\pm2)$. (b) The inset shows a portion of the ESM on the aluminum foil exposed to 70% ethanol overnight. The initial dimension of the ESM was equal to the aluminum foil before the exposure. The SEM image of the ESM shows that the membrane has lost its porosity after rinsing with 70% ethanol in a Petri dish. (c) Rinsing the ESM with 96% ethanol and immediately washing with PBS prevented the extensive dissolution of PMMA and protected the porous structure of the ESM. However, the ESM became a little crumpled, and the fibers were deformed. (d) The SEM image of the EMS embedded inside the microchip. Due to a small amount of ethanol, the structure of the fibers embedded into the microchip did not change significantly after rinsing with 70% ethanol. The inset demonstrates the image of the microchip with two inlets and two outlets (the grid of the white lines shows the embedded membrane inside the device).

washed with PBS to prevent extensive dissolution of PMMA and to protect the porous structure of the ESM. However, the fibers deformed, and the ESM became a little crumpled [Fig. 2(c)]. Nevertheless, when the ESM was integrated into the microchip, rinsing with 96% ethanol did not significantly deform the structure of the fibers, and the porosity of the ESM was preserved [Fig. 2(d)].

As the microchannel was small, the washing process was performed faster than that in a Petri dish, and a smaller amount of 96% ethanol was required for the rinsing process. Therefore, the solvent had less time to dissolve the material of the ESM, and the small amount was not sufficient to distort the ESM significantly. In addition, the ESM in the microchip was restricted by the surrounding walls, which prevented the fiber bending as a result of the PMMA dissolution. The result of FTIR analysis in Fig. 3 indicated that there was no new chemical bond in the sample after being exposed to 70% ethanol overnight at room temperature. Nevertheless, washing the ESM with the ethanol/water mixture made it hydrophilic as the hydroxyl groups of the ethanol/water mixture oriented the hydrophilic tails of the polymer chains toward the surface. Hydrophilicity enhanced cell adhesion and subsequently made the ESM suitable for cell culture. Although various methods have been developed to modify the hydrophobicity of the PDMS surface, these methods are time-consuming and require expensive or specialized equipment.³⁸ Moreover, in some surface modification methods, the level of the hydrophilicity only slightly improves or the morphology of the surface may change dramatically.³⁹ Here, we presented a simple method to increase the hydrophilicity of the ESM without changing the porosity of the membrane while preventing the fibers from dissolving.

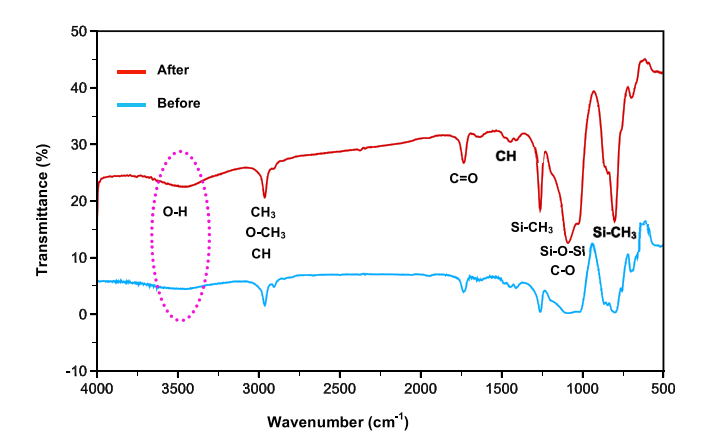


FIG. 3. FTIR and the functional groups of the ESM before and after being exposed to 70% ethanol overnight. The data illustrate that there is no new chemical bond in the sample after 24h of ethanol exposure. It is worth noting that washing the ESM with the ethanol/water mixture made the ESM hydrophilic as the hydroxyl groups (O-H) of the ethanol/water mixture oriented the hydrophilic tails of the polymer chains toward the surface.

B. Cell culture on the ESM in a 24-well plate

Human lung cancer epithelial cells (A549) were cultured on the ESM pieces located in a 24-well plate. As a control group, the same total number of cells (i.e., 4.8×10^4 cells) was cultured in a commercial treated 24-well plate (Jet Biofil®, Guangzhou Jet Bio-Filtration Co., China). A colorimetric analysis based on MTT assay was used to evaluate the cell viability and cell growth. For each experiment, the values of optical density (OD) obtained from the spectrophotometer for the background (blank) and the samples at the wavelength of 590 nm were recorded. Each experiment was conducted at least three times in a 24-well plate (for each experiment, four pieces of ESMs were located in four different wells). To compare the results, the ESM-to-control cell viability ratio (ϕ) was calculated as follows:

$$\Phi = (OD_{ESM} - OD_{background})/(OD_{control} - OD_{background}), \tag{1}$$

where OD_{ESM} is the OD of the cells cultured on the ESM, $OD_{background}$ is the OD of the background, and $OD_{control}$ is the OD of the control group (the cells cultured on the commercial well plate). Figure 4 shows the quantitative results of this comparison at the 2nd day, 4th day, and 6th day following the initial cell seeding. The reported results are based on an average of 12 samples for each experiment. These results confirmed the cell viability on the ESM and also demonstrated that the cell viability was significantly (P < 0.001, based on statistical T-test,

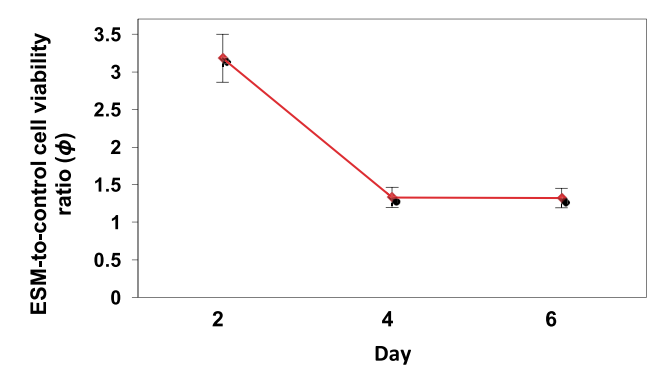


FIG. 4. Comparison of the cell viability on the ESM and the commercial well plate (control) using MTT assay. The reported results are based on an average of 12 samples for each experiment. For the first 2 days, the cell viability was significantly higher (P < 0.001, based on the statistical T-test, N = 12) on the ESM compared to that on the control group (i.e., the commercial treated 24-well plate). As the cells reached the plateau phase of growth, no significant differences were observed for the 4th day and 6th day.

N=12) higher on the ESM compared to that on the control group (i.e., the commercial treated 24-well plate) for the first 2 days. The large surface area to volume ratio of the ESM provided larger space for cell viability. It suggests that cell growth was faster on the ESM compared to the commercial plate within the first 48 h. In the subsequent days, the cells reached a plateau phase in growth. Accordingly, no significant differences were observed on the cell viability at the following days (i.e., 4th day and 6th day). This signifies that under the same cell density, the ESM provides a better scaffold for cell culture compared to commercial plates.

In the cell fixation process, the dehydration in the ethanol gradient (60%, 70%, 80%, 90%, and 100% ethanol) caused PMMA to dissolve and cover the surface of both fibers and cells as shown in Fig. 5(a). Therefore, the image of cell growth over time was not clear enough for a detailed investigation. It is suggested that for all the electrospun scaffolds and the fibers containing PMMA, the alcohol gradient should be discarded to prevent the dissolution of the fibers. In order to detect the cell images more clearly, in another test, the ethanol gradient was discarded, and the cells were incubated only in 4% glutaraldehyde for 3 h. This protocol provided clearer cell images, which are shown in Fig. 5(b). After 48 h, the cells adhered well to the ESM. After 72 h, the cells gradually proliferated and created a 3D-like monolayer of the cells. After 120 h, the cells became flattered and covered more areas of the ESM. For the alveolar

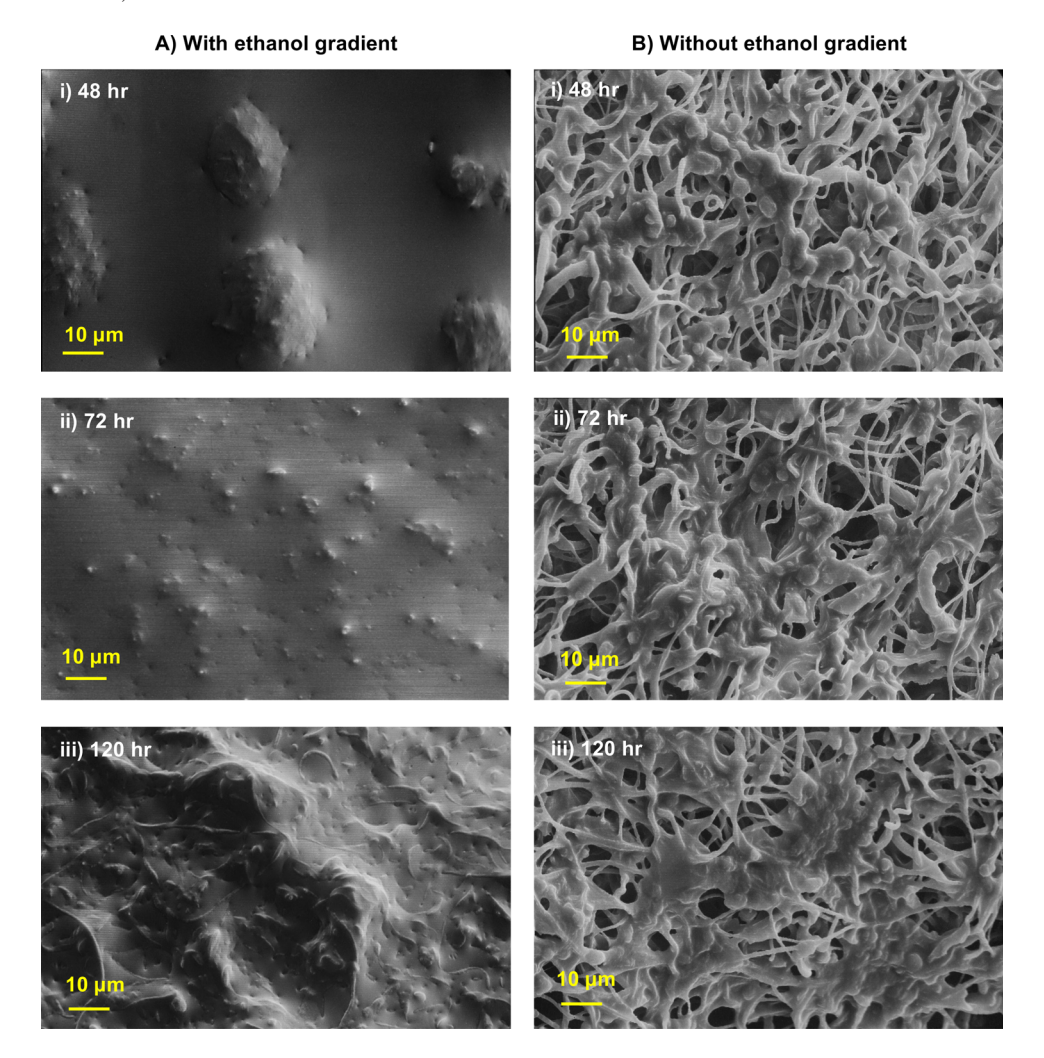


FIG. 5. (a) SEM images of cells on the ESM dehydrating with an ethanol gradient that dissolved the PMMA of the scaffold and covered the surface of the scaffold and cells. It is impossible to detect the cell in this group of the sample after (i) 48 h, (ii) 72 h, and (iii) 120 h of cell seeding. (b) The cell fixation by glutaraldehyde on the ESM. (i) After 48 h, the cells adhered well to the ESM. (ii) After 72 h, the cells gradually proliferated and created a 3D-like monolayer of the cells. (iii) After 120 h, the cells became flattered and covered more areas of the ESM.

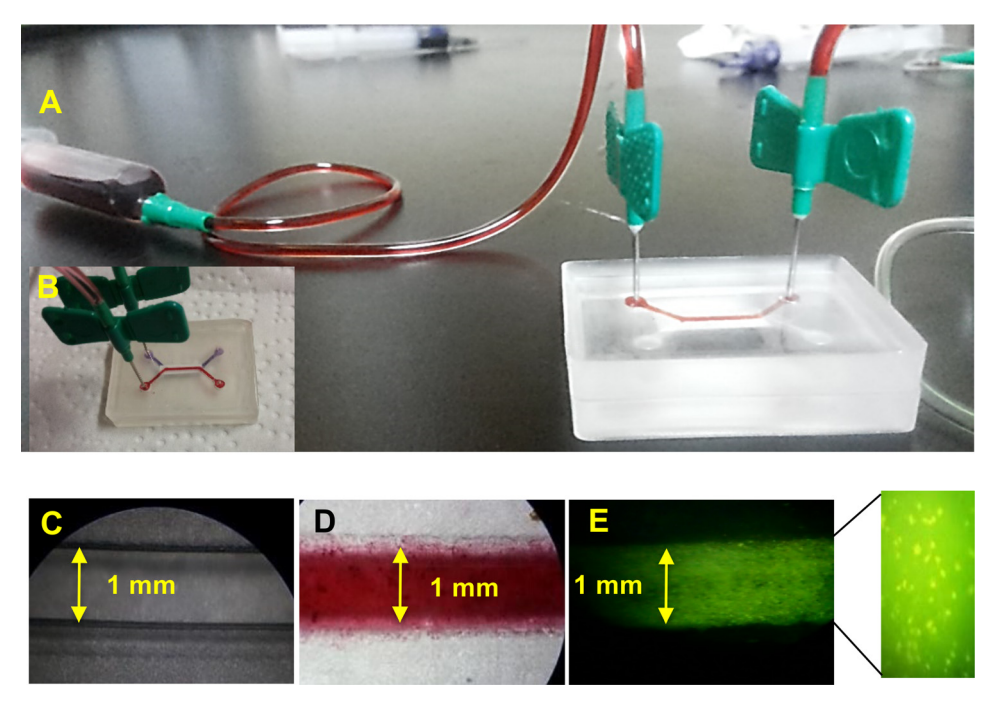


FIG. 6. Cells were successfully cultured on the ESM-embedded microfluidic device. (a) Various values of the flow rate ranging from 1 to $50 \,\mu$ l/min were introduced into the microchannel. (b) To evaluate the efficiency of the bonded layers, two liquids with different colors were injected into each microchannel at different flow rates. (c) Microscopy image of the ESM embedded into the microchip. (d) No leakage was observed in the microchannels after injecting a red-colored liquid. (e) The fluorescence image of the cells cultured on the ESM embedded into the microchip.

lung cells, which form a monolayer configuration in the body, this modified hydrophilic membrane provides a better microenvironment with surface buckling and dips on the order of the cell diameter. The *in vivo* similarity is highly desired for cell culture scaffolds, and it is indeed the main advantage of the ESM fabricated in this study. Cells sense the surface roughness and respond to it by changing their features, which in turn impact the cell reactions.⁴⁰

C. Cell culture in the microchip

A microchip with three layers, including a membrane and two PDMS layers, consisting of two microchannels, was fabricated as explained in Sec. II C. A red-colored liquid (pen ink) was introduced into the microchip with different flow rates ranging from 1 to 50μ l/min, and no leakage was detected, Fig. 6(a). This range of flow rates was much higher than that in similar applications as reported in the literature $(0.5 \mu$ l/min). A series of experiments with two liquids with different colors was carried out to evaluate the efficiency of the bonded layers, Fig. 6(b). Accordingly, ESMs with various thicknesses ranging from 20 to 120μ m were embedded into the microfluidic device under the leak-free conditions, Figs. 6(c) and 6(d). The cells were cultured successfully on the ESM-embedded microchip as shown in Fig. 6(e).

When the cells were cultured in the microchip without ethanol rinsing, the cells did not attach to the hydrophobic fibers but were trapped in the hydrophobic pores of the ESM. For a very small cell seeding density, 1×10^6 cells/ml, most of the pores captured only a single cell, Fig. 7(a). As shown in Fig. 7(b), 48 h after cell seeding, some of the cells proliferated and aggregated with each other, but the rest failed to proliferate. As the cells did not stick to the hydrophobic fibers, they aggregated with each other and formed some 3D clusters after 72 h, as shown in Figs. 7(c) and 7(d). Zuchowska *et al.* generated cell spheroids of A549 using microwells and reported that the cross-sectional area of the generated spheroid diameter remained unchanged in the following days.⁴² However, in our platform, the cross-sectional area of the cell cluster increased

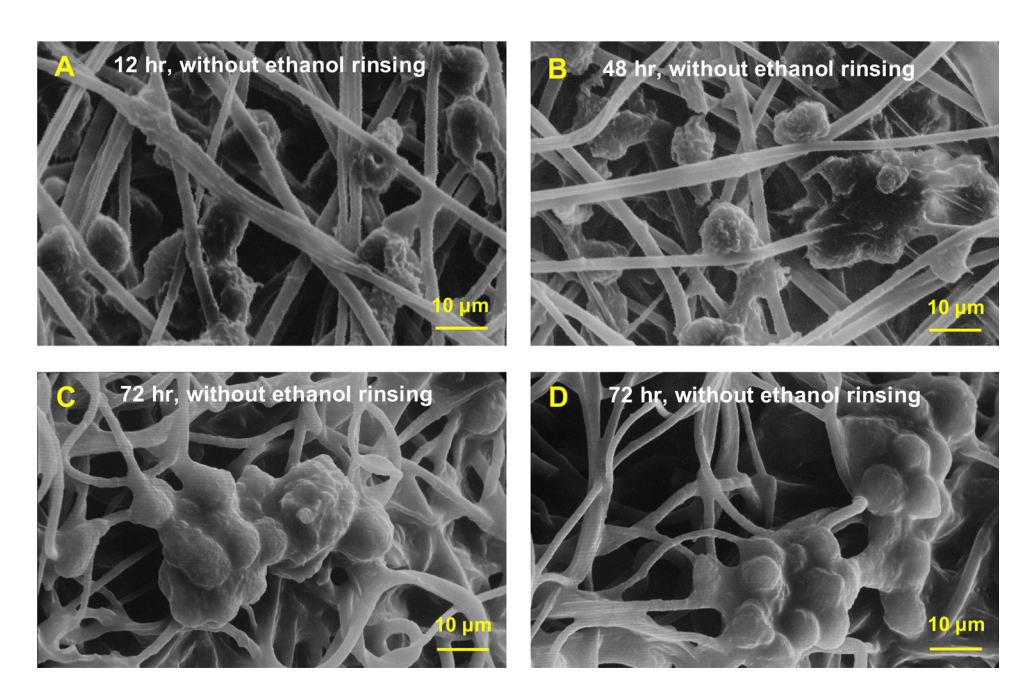


FIG. 7. The cells cultured in the microchip without ethanol rinsing did not attach to the hydrophobic fibers. (a) The cells were trapped in the hydrophobic pores of the ESM after 12 h. (b) 48 h after cell seeding, some of the cells proliferated and aggregated with each other, but the rest failed to proliferate. (c) and (d) after 72 h, the cells aggregated to each other and formed 3D clusters.

gradually over time. The cell aggregation is affected by the matrix proteins in culture medium and the capacity of integrins in the cell membranes to bind to the ECM.⁴³ We did not add any matrix proteins to the culture medium, and A549 cells cannot produce adhesive proteins.⁴² As such, we presume that the volume of the integrin in the cell membranes of A549 was high enough to attach the proliferated cells. However, Zuchowska *et al.* claimed that additional adhesive protein was necessary for A549 cells to aggregate.⁴² This inconsistency indicates that the process of aggregation is different when 3D cell clusters are generated from a single cell (as observed in our experiment) compared to the aggregation through the cellular accumulation (corresponding to Zuchowska's research⁴²).

Washing the membrane with 70% ethanol made it hydrophilic so that the cells tended to adhere to the fibers. These results are shown in Fig. 8(a) for a cell seeding density of 1×10^6 cells/ml after 48 h. Here, the cells aggregated to each other or attached to the hydrophilic fibers of the ESM. Most notably, the process led to various growth structures, i.e., 2D monolayer, single cell, and 3D cell cluster, after 72 h as shown in Fig. 8(b). The cells on the hydrophilic ESM tended to expand the uropod toward the neighboring cells [red arrows in Fig. 8(c)] and also toward the hydrophilic fibers [yellow arrows in Fig. 8(c)]. On the other hand, the cells on the hydrophobic ESM, without ethanol rinsing, tended to expand the uropod toward each other only, which is shown by red arrows in Fig. 8(d). There is no extended uropod toward the fibers as they are hydrophobic. Accordingly, expanding the uropod toward the hydrophilic fibers may restrict the cells to a monolayer structure.

The formation of each structure, i.e., monolayer, single cell, and 3D cell cluster, depends on the spatial gradient of the ESM hydrophobicity. The coexistence of these different modes of cell aggregation in a single membrane under the same culture conditions is unique, showing great promise especially for pharmacological study. Single-cell analysis is very critical for studying complex biological processes. However, in monolayer structures, the boundaries of the cells are protected by the adjacent cells. Consequently, the responses of the cells to the external signals differ from those of a single cell. It was shown that cells aggregated in a 3D configuration could better recapitulate the gradients of oxygen and nutrients to the cells similar

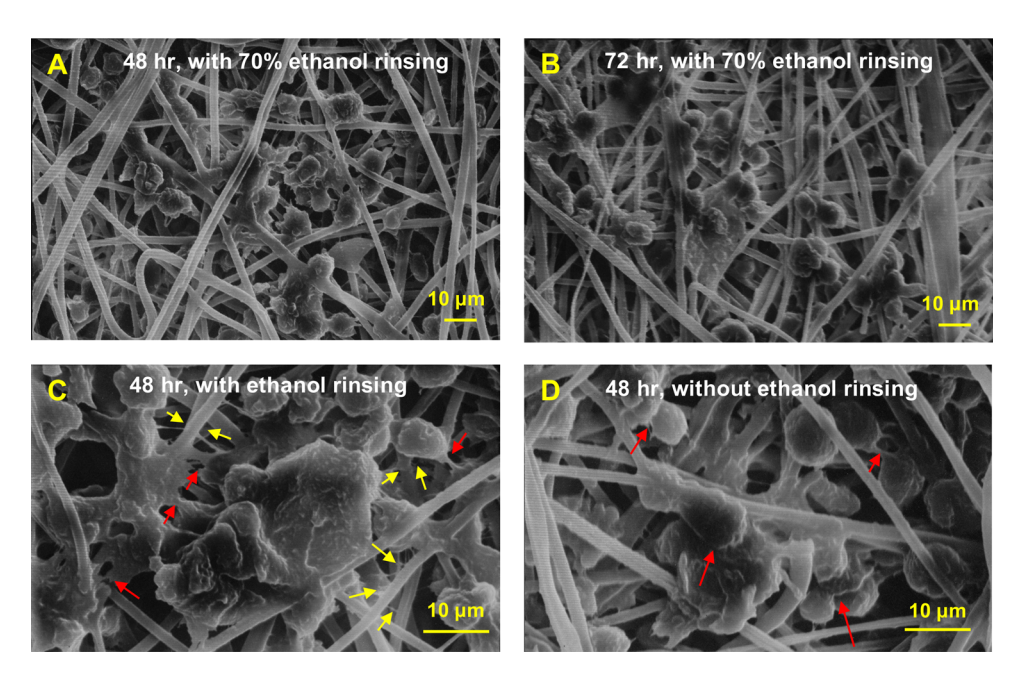
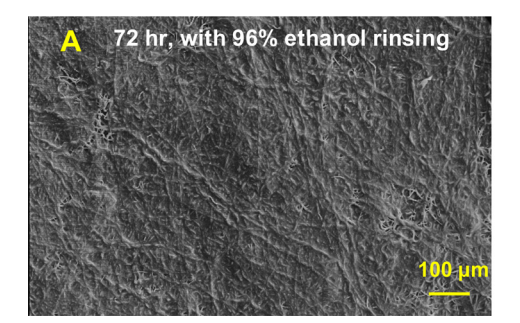


FIG. 8. (a) Rinsing the ESM with 70% ethanol made it hydrophilic. The cells attached to the hydrophilic fibers of the ESM or aggregated with each other after 48 h. (b) Various growth structures, i.e., monolayer, single cell, and 3D cell cluster, were generated on the hydrophilic ESM after 72 h. (c) The cells on the hydrophilic ESM tended to expand the uropod toward both the adjacent cells (red arrows) and the hydrophilic fibers (yellow arrows). (d) As indicated by red arrows, the cells on the hydrophobic ESM tended to expand the uropod toward each other only. Due to the hydrophobicity of the membrane, there was no extended uropod toward the fibers.

to *in vivo* tumor aggregates.² Coexistence of all the three configurations in a single microchip allows for the investigation of the complex cell-cell interaction under the same experimental conditions.

The surface modification was done by the ethanol/water mixture. As such, the level of hydrophobicity of the ESM was a function of the concentration of the ethanol in the mixture. Accordingly, two concentrations of ethanol in water, i.e., 70% and 96%, were used to modify the microchip embedded with ESMs. In both cases, a cell pellet containing 4×10^6 cells was seeded into the microchips. As shown in Fig. 9(a), after 72 h, a relatively uniform monolayer of the cell was created on the ESM rinsed with 96% ethanol, while the condition of the cells on the ESM rinsed with 70% ethanol was not proper for a monolayer cell structure after the same period [Fig. 9(b)]. These results indicate that rinsing the ESM with 96% ethanol can create a more spatially unvarying wetting state because the cell monolayer is more uniform than that with 70% ethanol.

The interaction between fibers and cells has been extensively studied for different cells¹⁸ and was not the focus of the present study. In this study, we examined the possibility of cell



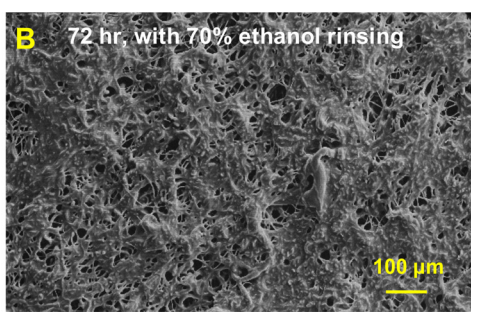


FIG. 9. The level of hydrophobicity of the ESM was a function of the concentration of ethanol in the mixture. For a cell pellet containing 4×10^6 cells after 72 h, (a) a relatively uniform monolayer of the cell was created on the ESM rinsed with 96% ethanol, while (b) the condition of the cells on the ESM rinsed with 70% ethanol was not proper for a monolayer cell structure.

culture on the ESM fabricated from the high PDMS content and incorporated into a PDMS microfluidic device. The results indicated that the proposed ESM has several advantages over the existing planar membrane. The substrate had 3D topography and offered ECM-free cell attachment, and the fabrication method was simple and inexpensive. We demonstrated that the cells could be immobilized in the platform either on hydrophilic fibers treated with ethanol or within the hydrophobic micro-pores of the ESM. This ability makes the ESM suitable for both anchorage-dependent and anchorage-independent cell types. In addition, this platform provides a unique opportunity to generate single cells, monolayer cells, and 3D cell clusters in the same microenvironment for further studies such as investigating cell-cell interactions and mechanisms of anti-cancer drug resistance.

IV. CONCLUSIONS

In this study, a cost-effective and straightforward microfluidic platform was introduced for cell culture. Using an electrospinning technique with PDMS and PMMA as carrier polymers, robust membranes with the thickness ranging from 20 to 120 µm were fabricated and subsequently embedded in a microfluidic device. A protocol for efficient sealing with simple oxygen plasma bonding was presented. Strong bonding without any leakage, even with a high flow rate of 50 µl/min, was obtained. This relatively hydrophobic ESM became hydrophilic by washing with the ethanol/water mixture and eliminated the need for ECM coating or other surface treatment. The method promises a cost-effective 3D scaffold for cell culture which is the main advantage of the proposed ESM. In a conventional well plate, the membrane shrank more than $70 \pm 4\%$ when exposed to 70% ethanol overnight because of dissolving PMMA. The dissolution of PMMA negatively affected the porosity of the membrane. As such, we proposed a simple protocol to increase the hydrophilicity of the microchip embedded with ESM without changing the porosity of the membrane, while preventing the fibers from dissolving. The proposed platform provides the ability of the growth of a single cell, a monolayer, and a 3D cell cluster. The coexistence of all three configurations in a single microchip allows the parallel investigation of cell-cell interactions on growth and reproduction of cells as well as drug resistance. Such a platform can also be helpful for anti-cancer drug development before introducing a new therapeutic agent for animal study or human clinical trials.

```
<sup>1</sup>N.-T. Nguyen, M. Hejazian, C. H. Ooi, and N. Kashaninejad, Micromachines 8, 186 (2017).
```

²N. Kashaninejad, M. R. Nikmaneshi, H. Moghadas, A. K. Oskouei, M. Rismanian, M. Barisam, M. S. Saidi, and B. Firoozabadi, Micromachines **7**(8), 130 (2016).

³K. Moshksayan, N. Kashaninejad, M. E. Warkiani, J. G. Lock, H. Moghadas, B. Firoozabadi, M. S. Saidi, and N.-T. Nguyen, Sens. Actuators, B **263**, 151–176 (2018).

⁴N. Kashaninejad, M. J. A. Shiddiky, and N.-T. Nguyen, Adv. Biosyst. 2(3), 1700197 (2018).

⁵M. Barisam, M. Saidi, N. Kashaninejad, R. Vadivelu, and N.-T. Nguyen, Micromachines 8(12), 358 (2017).

⁶J. De Jong, R. Lammertink, and M. Wessling, Lab Chip **6**(9), 1125–1139 (2006).

⁷K. B. Neeves and S. L. Diamond, Lab Chip **8**(5), 701–709 (2008).

⁸D. Huh, B. D. Matthews, A. Mammoto, M. Montoya-Zavala, H. Y. Hsin, and D. E. Ingber, Science 328(5986), 1662–1668 (2010).

⁹E. W. Young, M. W. Watson, S. Srigunapalan, A. R. Wheeler, and C. A. Simmons, Anal. Chem. 82(3), 808–816 (2010).

¹⁰N. Kashaninejad, N.-T. Nguyen, and W. K. Chan, Phys. Fluids **24**(11), 112004 (2012).

¹¹N. Kashaninejad, W. K. Chan, and N.-T. Nguyen, paper presented at the ASME 9th International Conference on Nanochannels, Microchannels, and Minichannels, Edmonton, AL, Canada (2011), Vol. 1, pp. 647–655.

¹²W. Chen, R. H. Lam, and J. Fu, Lab Chip **12**(2), 391–395 (2012).

¹³D. F. Stamatialis, B. J. Papenburg, M. Gironés, S. Saiful, S. N. Bettahalli, S. Schmitmeier, and M. Wessling, J. Membr. Sci. 308(1), 1–34 (2008).

¹⁴M. Haerst, V. Seitz, M. Ahrens, C. Boudot, and E. Wintermantel, paper presented at the 6th European Conference of the International Federation for Medical and Biological Engineering (2015).

¹⁵R. Xue, P. Behera, J. Xu, M. S. Viapiano, and J. J. Lannutti, Sens. Actuators, B **192**, 697–707 (2014).

¹⁶X. Wang, B. Ding, and B. Li, Mater. Today **16**(6), 229–241 (2013).

¹⁷D. I. Braghirolli, F. Zamboni, G. A. Acasigua, and P. Pranke, Int. J. Nanomed. 10, 5159 (2015).

¹⁸Z. Guo, J. Xu, S. Ding, H. Li, C. Zhou, and L. Li, J. Biomater. Sci., Polym. Ed. **26**(15), 989–1001 (2015).

¹⁹H. Moghadas, M. S. Saidi, N. Kashaninejad, A. Kiyoumarsioskouei, and N.-T. Nguyen, Biomed. Microdevices 19(4), 74 (2017).

²⁰K. Garg and G. L. Bowlin, Biomicrofluidics **5**(1), 013403 (2011).

²¹N. Higuita-Castro, C. Mihai, D. J. Hansford, and S. N. Ghadiali, paper presented at the ASME 2011 Summer Bioengineering Conference (2011).

- ²²Y. Liu, D. Yang, T. Yu, and X. Jiang, Electrophoresis **30**(18), 3269–3275 (2009).
- ²³E. Jo, M. C. Lim, H. N. Kim, H. J. Paik, Y. R. Kim, and U. Jeong, J. Polym. Sci., Part B: Polym. Phys. 49(2), 89–95 (2011)
- ²⁴P. Wallin, C. Zandén, B. Carlberg, N. H. Erkenstam, J. Liu, and J. Gold, Biomicrofluidics **6**(2), 024131 (2012).
- ²⁵S. Huang, C. S. Chen, and D. E. Ingber, Mol. Biol. Cell **9**(11), 3179–3193 (1998).
- ²⁶H. Wang, G. M. Riha, S. Yan, M. Li, H. Chai, H. Yang, Q. Yao, and C. Chen, Arterioscler., Thromb., Vasc. Biol. 25(9), 1817-1823 (2005).
- ²⁷E. W. Young, A. R. Wheeler, and C. A. Simmons, Lab Chip **7**(12), 1759–1766 (2007).
- A. Shamloo, N. Ma, M.-M. Poo, L. L. Sohn, and S. C. Heilshorn, Lab Chip 8(8), 1292–1299 (2008).
 H. Chung, C. K. Chan, T. S. Khire, G. A. Marsh, A. Clark, R. E. Waugh, and J. L. McGrath, Lab Chip 14(14), 2456-2468 (2014).
- ³⁰T. G. Vladkova, Int. J. Polym. Sci. **2010**, 296094.
- ³¹H. J. Chung and T. G. Park, Adv. Drug Delivery Rev. **59**(4–5), 249–262 (2007).
- ³²A. Martins, E. D. Pinho, S. Faria, I. Pashkuleva, A. P. Marques, R. L. Reis, and N. M. Neves, Small 5(10), 1195–1206 (2009).

 33S. Halldorsson, E. Lucumi, R. Gómez-Sjöberg, and R. M. Fleming, Biosens. Bioelectron. 63, 218–231 (2015).
- ³⁴D. Yang, X. Liu, Y. Jin, Y. Zhu, D. Zeng, X. Jiang, and H. Ma, Biomacromolecules **10**(12), 3335–3340 (2009).
- ³⁵H. Moghadas, M. S. Saidi, N. Kashaninejad, and N.-T. Nguyen, Drug Delivery Transl. Res. (to be published).
- ³⁶R. Hoogenboom, C. R. Becer, C. Guerrero-Sanchez, S. Hoeppener, and U. S. Schubert, Aust. J. Chem. **63**(8), 1173–1178 (2010). ³⁷S. K. Jewrajka, U. Chatterjee, and B. M. Mandal, Macromolecules **37**(11), 4325–4328 (2004).
- ³⁸S. H. Tan, N.-T. Nguyen, Y. C. Chua, and T. G. Kang, Biomicrofluidics **4**(3), 032204 (2010).
- ³⁹E. Yilgor, O. Kaymakci, M. Isik, S. Bilgin, and I. Yilgor, Appl. Surf. Sci. **258**(10), 4246–4253 (2012).
- ⁴⁰J. Y. Lim and H. J. Donahue, Tissue Eng. **13**(8), 1879–1891 (2007).
- ⁴¹D. Huh, H. J. Kim, J. P. Fraser, D. E. Shea, M. Khan, A. Bahinski, G. A. Hamilton, and D. E. Ingber, Nat. Protoc. 8(11), 2135 (2013).
- ⁴²A. Zuchowska, E. Jastrzebska, K. Zukowski, M. Chudy, A. Dybko, and Z. Brzozka, Biomicrofluidics 11(2), 024110
- ⁴³R.-Z. Lin, L.-F. Chou, C.-C. M. Chien, and H.-Y. Chang, Cell Tissue Res. **324**(3), 411–422 (2006).
- ⁴⁴F. Ye, J. Jiang, H. Chang, L. Xie, J. Deng, Z. Ma, and W. Yuan, Biomicrofluidics **9**(4), 044106 (2015).